

The Human and Mouse SLC25A29 Mitochondrial Transporters Rescue the Deficient Ornithine Metabolism in Fibroblasts of Patients With the Hyperornithinemia-Hyperammonemia-Homocitrullinuria (HHH) Syndrome

JOSÉ A. CAMACHO AND NATALIA RIOSECO-CAMACHO

Department of Pediatrics, University of California-Irvine, Irvine, California 92697

ABSTRACT: The hyperornithinemia-hyperammonemia-homocitrullinuria (HHH) syndrome is a disorder of the urea cycle (UCD) and ornithine degradation pathway caused by mutations in the mitochondrial ornithine transporter (ORNT1). Unlike other UCDS, HHH syndrome is characterized by a less severe and variable phenotype that we believe may, in part, be due to genes with redundant function to *ORNT1*, such as the previously characterized *ORNT2* gene. We reasoned that *SLC25A29*, a member of the same subfamily of mitochondrial carrier proteins as *ORNT1* and *ORNT2*, might also have overlapping function with *ORNT1*. Here, we report that both the human and mouse *SLC25A29*, previously identified as mitochondrial carnitine/acyl-carnitine transporter-like, when overexpressed transiently also rescues the impaired ornithine transport in cultured HHH fibroblasts. Moreover, we observed that, in the mouse, the *Slc25a29* message is more significantly expressed in the CNS and cultured astrocytes when compared with the liver and kidney. These results suggest a potential physiologic role for the *SLC25A29* transporter in the oxidation of fatty acids, ornithine degradation pathway, and possibly the urea cycle. Our results show that *SLC25A29* is the third human mitochondrial ornithine transporter, designated as *ORNT3*, which may contribute to the milder and variable phenotype seen in patients with HHH syndrome. (*Pediatr Res* 66: 35–41, 2009)

The hyperornithinemia-hyperammonemia-homocitrullinuria (HHH) syndrome (OMIM 238970), an autosomal recessive disorder of the urea cycle and ornithine degradation pathway, is caused by mutations in the mitochondrial ornithine transporter (ORNT1) (1,2). In general, patients with HHH syndrome have a later onset and milder clinical presentation compared with patients with other urea cycle disorders such as deficiency of ornithine transcarbamylase (OTC). Moreover, a salient feature of HHH syndrome is the marked clinical variability seen among patients carrying the same mutant *ORNT1* allele (3,4).

Biochemically, patients with HHH syndrome are characterized by chronic elevation in plasma levels of ornithine, episodic or postprandial hyperammonemia, and urinary excretion of homocitrulline and orotic acid (2). The chronic hyperornithinemia of HHH patients may be indistinguishable from the

plasma ornithine levels of patients with retinopathy secondary to a deficiency in ornithine aminotransferase (OAT) (2). Presenting symptoms for HHH patients may include liver dysfunction, coagulopathies, unexplained seizure activity, developmental and growth delay, academic difficulties, gait disturbances, and stroke-like episodes (1–4). The cognitive development of HHH patients may vary from normal intelligence to mild and severe mental retardation. In general, HHH patients are maintained on a protein restricted diet and supplemented with special formulas, citrulline and sodium phenylbutyrate.

We believe that the mechanisms of disease underlying the variable phenotype of patients with HHH syndrome may include differences in mitochondrial physiology, the existence of additional transporters with redundant function to *ORNT1*, and environmental or epigenetic factors (3). Recent evidence that additional factors may influence the clinical presentation and course of HHH syndrome or other mitochondrial carrier disorders is the observation of posttranslational modifications, such as lysine acetylation, of murine mitochondrial carrier proteins, and *Otc* (5). Furthermore, we identified human *ORNT2*, a functional retroposon that has overlapping functions with *ORNT1*, as a gene that may potentially modify the phenotype of patients with HHH syndrome (6). Both *ORNT2* and *ORNT1* belong to the mitochondrial carrier subfamily that includes the carnitine/acyl-carnitine transporter (*CACT*), *SLC25A29* and *SLC25A45*, a gene whose function is not known (7,8). By using an *in vitro* assay of ornithine metabolism in cultured fibroblasts of HHH patients, we previously showed that *CACT*, the mitochondrial transporter defective in a neonatal onset fatty acid oxidation defect, does not have overlapping function with *ORNT1* (6). For this work, we reasoned that *SLC25A29* may have overlapping functions with *ORNT1* given that it contains the mitochondrial signature sequence P²⁹FDT, a region that is conserved among several mitochondrial ornithine transporters from yeast to human (6). Interestingly, Sekoguchi *et al.* (9) previously reported that the murine *Slc25a29* functions as carnitine/acyl-carnitine trans-

Received September 22, 2008; accepted February 3, 2009.

Correspondence: José Angel Camacho, M.D., Department of Pediatrics, Division of Human Genetics and Metabolism, University of California, Irvine, 326 Sprague Hall, Irvine, California 92697; e-mail: jcamacho@uci.edu

Supported by Robert Wood Johnson Foundation Harold Amos Faculty Development Award.

Abbreviations: HHH, Hyperornithinemia-Hyperammonemia-Homocitrullinuria; **ORNT1 and Ornt1**, human and mouse mitochondrial ornithine transporter 1, respectively; **ORNT2**, human mitochondrial ornithine transporter 2; **ORNT3 and Ornt3**, human and mouse mitochondrial ornithine transporter 3, respectively

porter-like (CACL) and is up-regulated in response to partial hepatectomy and fasting.

In this report, we show that the human and mouse SLC25A29 transporters, but not the mouse Slc25a45, can rescue the defective ornithine metabolism in cultured fibroblasts of patients with HHH syndrome. In addition to being CACL, SLC25A29 is the third human mitochondrial ornithine transporter, designated as ORNT3; a gene that, although expressed at relatively low levels in the liver and highest levels in the CNS, may potentially modify the clinical phenotype of patients with HHH syndrome and perhaps be pharmacologically manipulated to compensate for a defective ORNT1.

METHODS

Total RNA isolation and real time PCR. We obtained total RNA (DNase treated, RNase-free) of different mouse tissues from CLONTECH (BD Biosciences, San Francisco, CA) and mouse cerebellar type II astrocytes from ATCC (Manassas, VA). To extract total RNA from cultured astrocytes, we used a combination of TRIzol reagent (Invitrogen, Carlsbad, CA) for isolation and Qiagen columns (Valencia, CA) for final purification and elution after on-column DNase I treatment. We performed reverse transcription with BioRad i-Script cDNA Synthesis kit (Hercules, CA) using 1 μ g of total RNA in accordance with the manufacturer's recommendation. By utilizing gene specific primers (Table 1) and cDNA as template, we amplified *Ornt1*, *Ornt3*, *Slc25a45*, *Cact*, *Otc*, and glyceraldehyde 3-phosphate dehydrogenase (*G3pdh*) from different mouse tissues. The complete open reading frame (ORF) and genomic structure of all amplified mouse genes used in designing PCR primers were obtained from the Mouse Ensemble website (www.ensembl.org/Mus_musculus/index.html).

For semi-quantitative RT-PCR, serial dilutions of cDNA from mouse tissues were made to determine amplification conditions within the exponential range for each target gene. A final amount of 200 ng cDNA was amplified at 96°C (1 min), [94°C (15 s), 62°C (30 s), 72°C (20 s)] \times 32 cycles and 72°C (20 s) for *Ornt1*, *Ornt3*, and *Slc25a45*, whereas 31 and 28 cycles were used for *Cact* and *G3pdh*, respectively. PCR products were quantified with an AlphaImager 2200 Documentation and Analysis System (Alpha Innotech Corporation, San Leandro, CA) at nonsaturating intensity and expressed as ratios of target gene to normalizer (*G3pdh*).

Next, we performed quantitative real-time PCR (qPCR) using qPCR primers for *Ornt1*, *Ornt3*, TATA box-binding protein (*Tbp*), and ribosomal

protein L27 (*Rpl27*). We obtained validated primers from Qiagen for *Ornt1* and *Tbp*. To confirm the identity of the amplified region of *Ornt1* and *Tbp*, we TA cloned (Invitrogen) and sequenced the amplified PCR products. The amplified regions of both sets of primers cross an intron-exon junction; namely, intron 6 that interrupts the amplified ORF of *Ornt1* (764–873 bp) and introns 7 and 8, which interrupt the amplified region of *Tbp* (608–722 bp). The primer sequences for *Ornt3* (JCUCI-135 and JCUCI-136) and *Rpl27* (JCUCI-141 and JCUCI-142) listed in Table 1 were obtained from the Massachusetts General Hospital and the Harvard School of Medicine Center for Computational and Integrative Biology website (pga.mgh.harvard.edu/primerbank/index.html). For *Ornt3*, the primers corresponded to the ORF region covering 36 to 109 bp (introns 2 and 3); whereas, for *Rpl27*, the primers corresponded to the ORF region covering 64 to 164 bp (intron 3). Optimization of each primer pair was carried out using serial dilutions and a range of annealing temperatures. The amplification efficiency of all primers was close to 1.0. We carried out first strand synthesis in duplicate reaction volume as mentioned earlier for RT-PCR. All samples were transcribed at the same time to minimize variation. We obtained nucleic acid concentrations on each cDNA sample and used 100 ng of cDNA template in each 25 μ L qPCR reaction using the iQ SYBR Green Supermix (BioRad) in accordance with the manufacturer's recommendation. A final primer concentration of 500 nM was used in all reactions. We normalized C_T (threshold cycle) results with two different housekeeping genes, *Tbp* and *Rpl27*. As documented by other investigators, we observed that, although *Tbp* and *Rpl27* produced a relatively constant expression across mouse tissues, slight differences between reference genes yielded differences in relative quantification among tissues after normalization and comparison to the heart, which was used as a calibrator (10).

Generation of mouse and human expression constructs. We first cloned the wild-type human and mouse ORNT3 cDNAs into the EcoRI/NotI site of pcDNA3.1 (Invitrogen). We next generated the N-myc (EQKLISEEDLL)-tagged human and mouse ORNT3 and mouse UCP-like (UniGeneMm.202653) constructs, the latter which served as a negative control, using the primers outlined in Table 1 and a pcDNA3.1 backbone as previously published (6). To generate both tagged and untagged *Ornt3* and *ORNT3* constructs, we used the mouse AA445192 (1,400 bp with ORF = 918 bp) and human BE791151 (1,440 bp with ORF = 909 bp) cDNAs as templates, respectively. For the mouse *Slc25a45* construct, we used a 1,453 bp cDNA (AW988159, ORF = 864 bp) obtained from Invitrogen and subcloned it into the EcoRI/NotI site of pcDNA3.1. The mouse UCP-like (ORF = 310aa) N-myc construct was generated in a one-step RT-PCR (Qiagen) reaction with mouse liver total RNA as a template following the manufacturer's recommendations. The mouse *Cact* expression construct has been previously reported (6). All constructs were sequenced as previously published (6).

Transfections, ornithine transport assay, and indirect immunofluorescence. For these experiments, we used established transformed primary

Table 1. Primer combinations for RT-PCR, qPCR, and expression constructs

Gene ID	Primer sequence*
<i>Ornt1</i>	CAGAATGCAGCTGCTGGTTCCTTTG GATACTCAGGAAGGTCCTGACGAG
<i>Ornt3</i>	GACTTCCTGGCTGGATGCGCC CAGCAGATGACACACTGAATGGCGCC
<i>Slc25a45</i>	GGTCAACTCCGTCCTGTTCGGAGTG CATTCTAACGTAGGAGTGCTCTCTC
<i>Cact</i>	GAGGATGAACTTAGCTACCCA GATCCGAGGCACGCTGAGGTC
<i>Otc</i>	GGTTATGAGCCAGATCCTAATATAGTC GACTTATTCTATTGCTAAAGAACAGAGG
<i>G3pdh</i>	GCTGTGGGCAAGGTCATCCAGAG CATGTAGGCCATGAGGTCCACCAC
JCUCI-135	TGTGGCAGGTGTGATCGTG
JCUCI-136	GTGAGTCCATTAGTGGCGA
JCUCI-141	AAAGCCGTCATCGTGAAGAAC
JCUCI-142	GCTGTCACTTTCCGGGGATAG
N-myc-ORNT3	CCCAAGCTTACCATGGAGCAGAAGCTGATCTCCGAGGAGGA CCTGCTGATGGCGCTGGACTTCTGGCTGGA ATAAGAATGCGGCCGCTCACAGGCTGGAGGGCTGCGCCAGG GCAGGCCCGCAGG
N-myc-Ornt3	CCCAAGCTTACCATGGAGCAGAAGCTGATCTCCGAGGAGGA CCTGCTGATGGCGCTCGACTTCTGCGTGGATGC ATAAGAATGCGGCCGCTCACAGACTGGAAGGCTGGGAGGGCAGGCCAGC
N-myc-UCP-like	CCCAAGCTTACCATGGAGCAGAAGCTGATCTCCGAGGAGGA CCTGCTGATGGATTTTGTGTGGGGCC ATAAGAATGCGGCCGCTCATGTGAGCAGGCTCTGCGTGAGCCTCAGCACAGCCTC

All primers are in the 5' to 3' sequence.

* For each pair, top sequence is forward primer and bottom sequence is reverse primer.

fibroblasts that carry the *ORNT1-F188Δ* allele, which produces an unstable protein, or the wild-type *ORNT1* allele, which served as a positive control (1). The UCI Institutional Review Board approved the use of human fibroblast cell lines. We cultured National Institutes of Health-3T3 fibroblasts and mouse cerebellar type II astrocytes in media containing DMEM, sodium pyruvate (1 mM), and 10% FCS. We performed electroporation, the ornithine transport assay, and immunofluorescence as previously described (6,11). Briefly, in the ornithine incorporation assays, transfected cells plated on glass coverslips were incubated for 6 h at 37°C in earle's balanced salt solution containing 0.1 μCi/mL each of ³H-leucine [L-(3,4,5-³H(N)), 173 mCi/mmol] and ¹⁴C-ornithine [L-(1-¹⁴C), 47.70 mCi/mmol] (Perkin Elmer, Boston, MA). The final ornithine concentration of 2.1 μM is below the K_m obtained for the purified human ORNT1 and cultured wild-type fibroblasts (220 μM) and human liver (80 μM) (8,12). For transient transfection studies, we assayed three to six wells per transfected plasmid and expressed results as mean ± SD. We expressed the ability to incorporate ¹⁴C-ornithine into protein as glutamate and proline relative to total protein synthesis (leucine-³H) as ¹⁴C/³H ratio. We analyzed data using the unpaired *t* test and presented our results in graphs as percent increase compared with control (untransfected) cells. Transfection efficiency varied between 25 and 30%.

RESULTS

Functional characterization of SLC25A29 (ORNT3). Previously, we hypothesized that both the *SLC25A29* and *SLC25A45* were potential genes with overlapping function to *ORNT1* based on phylogeny and the conservation of amino acid sequences P²⁹-F/L-D-T-Xaa-K-V-R/K (6). To test our hypothesis, we studied whether the human and mouse *SLC25A29* constructs and murine *Slc25a45* could rescue the deficient ornithine metabolism by using an established ornithine transport assay in transformed skin fibroblasts from control and HHH patients (6). For these experiments, we used the mouse *UCP-like* gene and *Cact* as negative controls and the human N-myc-*ORNT2* and mouse N-myc-*Ornt1* (wild-type) constructs as positive controls (6). Results from overexpression studies shown in Figure 1A clearly demonstrate that both the N-myc-tagged human *SLC25A29* and mouse *Slc25a29* constructs rescue the deficient ornithine transport by approximately 5-fold relative to untransfected HHH patient fibroblasts. Similar results were obtained using the untagged *SLC25A29* (data not shown) and *Slc25a29* (Fig. 1B) constructs. Hence, *SLC25A29*, hitherto also known as *CACL*, was identified as the third human mitochondrial ornithine transporter, ORNT3. Conversely, ornithine incorporation assay results in Figure 1B illustrate that neither the mouse *Cact*, *Slc25a45* nor *UCP-like* protein (data not shown) is capable of restoring the ornithine transport that is deficient in cultured HHH fibroblasts.

Concomitant with ornithine transport studies, we performed immunofluorescence to confirm that both the human and mouse N-myc-tagged ORNT3 proteins target to the mitochondria. Wild-type N-myc-tagged *Ornt1* served as a positive control. Results shown in Figure 2 demonstrate that both the human ORNT3 (data not shown) and mouse *Ornt3* transporters have a normal mitochondrial targeting pattern as evidenced by its localization in multiple, elongated, cytoplasmic structures that coincide with the location of MitoTracker-labeled mitochondria.

Comparison of Ornt3, Slc25a45, Ornt1, and CACT protein structure. In humans, the subfamily of mitochondrial carrier proteins that includes ORNT1, ORNT2, CACT, SLC25A45, and ORNT3 is characterized by the transport of

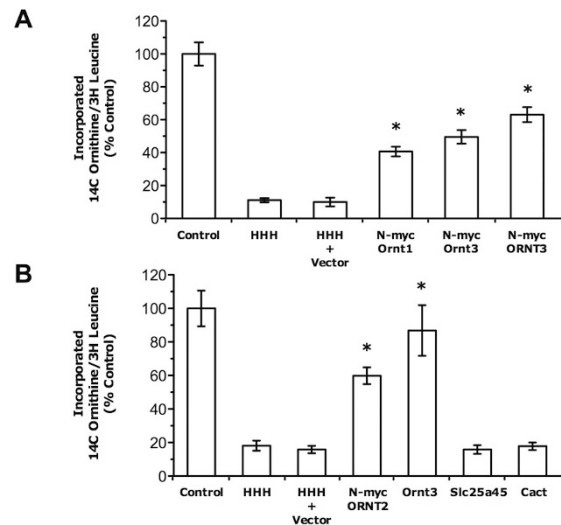


Figure 1. Transient expression of human and mouse *ORNT3* constructs restore ornithine metabolism in cultured HHH fibroblasts. Transformed HHH fibroblasts carrying the nonfunctional *ORNT1-F188Δ* allele were used to study the ability to incorporate ¹⁴C-ornithine and ³H-leucine 48 h after electroporation. The data are expressed as the ratio of ¹⁴C/³H in precipitated protein and represent the mean ± SD. For all studies, we electroporated fibroblasts with 25 μg of N-myc tagged or untagged construct or empty vector (pcDNA3.1). (A) Graph compares the ornithine incorporation of untransfected control and HHH-F188Δ fibroblasts vs. HHH-F188Δ fibroblasts transfected with either vector, N-myc tagged murine *Ornt1*, *Ornt3*, or human *ORNT3* constructs. (B) Data show the ornithine metabolism of untransfected control and HHH-F188Δ fibroblasts vs. HHH-F188Δ fibroblasts transiently transfected with either vector, N-myc tagged human *ORNT2* or untagged mouse *Ornt3*, *Slc25a45*, or *Cact* constructs. Data represent six separate experiments with four measurements per data point per experiment. **p* < 0.05 vs. HHH + vector.

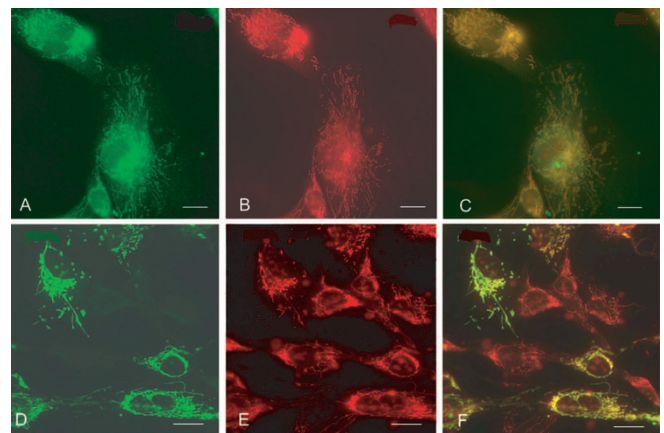


Figure 2. Ornt3 is localized to the mitochondria. HHH-F188Δ cells overexpressing mouse N-myc-*Ornt3* (A–C) or N-myc-*Ornt1* (D–F) transporter were prelabeled with MitoTracker (B and E), which stains mitochondria red, and processed for indirect immunofluorescence using a monoclonal FITC-labeled anti-myc antibody (A and D). Overlay of the images (C and F) show the mitochondrial localization of both transporters. Bars denote 20 μm.

charged amino compounds such as ornithine, arginine, carnitine, and citrulline (8). Interestingly, in the mouse, the *Ornt2* gene is nonfunctional because it is not translated unlike the functional *ORNT2* present in the human and other mammalian species (6). Moreover, there is very high amino acid sequence similarity between human and mouse orthologues of this

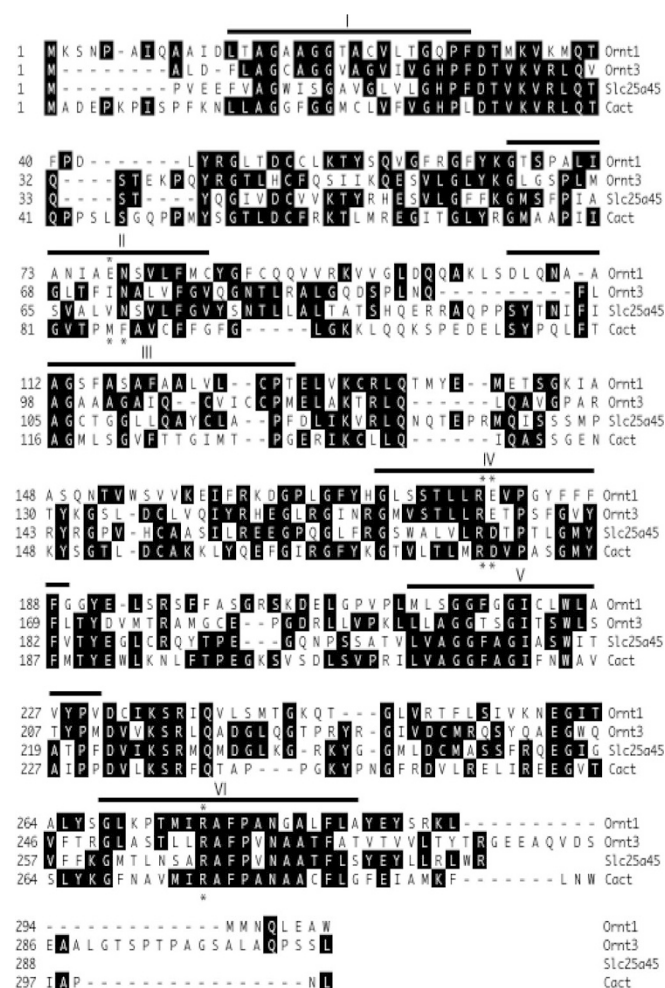


Figure 3. Sequence alignment of the mouse mitochondrial carrier proteins Ornt1, Ornt3, Slc25a45, and Cact. Amino acids that are conserved relative to Ornt1 are highlighted in black. Filled lines (Roman numerals I–VI) indicate the predicted TMDs. The mitochondrial carrier signature motif [P-h-D/E-Xaa-h-K/R-Xaa-K/R-(20–30aa)-D/E-G-(4Xaa)-a-K/R-G (h, hydrophobic; Xaa, any amino acid)] begins in the region of the first, third, and fifth TMD of each protein. Amino acids in asterisks (*) for Ornt1 and Cact are predicted to be involved in solute recognition.

subfamily. Given that Ornt3 has overlapping functions with Cact and Ornt1, we thought it important to compare the protein structure of four members of this subfamily of mitochondrial transporters. As shown in Figure 3, comparison of the amino acid sequences of the mouse Ornt1, Cact, Ornt3, and Slc25a45 demonstrate that the regions of the first hydrophilic loop and the fourth, fifth, and sixth transmembrane domains (TMDs) contain the highest number of conserved amino acids. Interestingly, recently published reports have demonstrated that the region previously thought to be the beginning of the first, third, and fifth hydrophilic loop (after the proline in the mitochondrial motif) actually forms part of a TMD (8). At the amino acid level, Ornt3 is 34% identical to Ornt1 and 37% identical to Cact (9). Most importantly, some of the conserved amino acids (Arg and Asp/Glu) in the fourth and sixth TMD that are thought to play a potential role in solute recognition in Cact and Ornt1 are also conserved in Ornt3 (13). In the case of human ORNT1, several of these

conserved amino acids (Arg¹⁷⁹, Glu¹⁸⁰, and Arg²⁷⁵) were mutated in patients with HHH syndrome (1,8). Conversely, though Glu⁷⁷ has been implicated as part of the ornithine binding site of Ornt1, there is no such conserved amino acid in the second TMD of Ornt3 (13). Lastly, similar to Ornt1 and most mitochondrial carrier proteins, Ornt3 has consensus sites for serine/threonine phosphorylation by protein kinases, such as PKC (S/T-Xaa-R/K) (3).

Finally, examination of the genomic structure of the *Ornt3* revealed that it has three introns interrupting the ORF and, surprisingly, the region corresponding to TMD II–VI is contained within a single exon, exon 4. This is in sharp contrast to *Ornt1*, *Cact*, and *Slc25a45* that have several introns (five for *Ornt1* and *Slc25a45*; eight for *Cact*) that interrupt the ORF of the structural genes of these three transporters.

mRNA tissue distribution of mouse Ornt3. We initially used semi-quantitative RT-PCR to investigate the mRNA tissue distribution of *Ornt3* vs. that of *Ornt1*, *Cact*, and *Slc25a45*. We compared CNS derived tissues (whole brain, cerebellum, cortex, hypothalamus, and hippocampus) with peripheral tissues such as liver, kidney, heart, and testis. As shown in Figure 4, the expression of *Ornt1* is much more predominant in the liver, kidney, and testis when compared with the CNS and the heart; whereas, for *Ornt3*, after normalization with *G3pdh*, the level of mRNA expression in brain derived tissues and is higher relative to heart, liver, kidney, and testis. The distribution of *Cact* mRNA follows the pattern expected for tissues heavily dependent on fatty acid oxidation such as the liver, kidney, testis, and heart. Interestingly, the mRNA distribution pattern of the *Slc25a45* gene was similar to that of *Cact*, except for the heart that exhibited low *Slc25a45* expression. *Slc25a45* was also previously shown to be expressed in brain tissues (cortex and pons) of the rat (7). Finally, using similar RT-PCR conditions, we obtained a restricted expression in the liver for *Otc* (data not shown).

Given the relatively higher level of *Ornt3* expression in CNS derived tissue, we next performed a more accurate determination using quantitative real time PCR. For these experiments, we obtained the relative quantification of *Ornt3* and *Ornt1* using *Tbp* and *Rpl27* as reference genes and the heart as a calibrator. Results shown in Figure 5 demonstrate marked *Ornt1* expression in the liver (27-fold–37-fold) and kidney (~6-fold) relative to the heart, CNS tissues, and cultured murine astrocytes. A similar expression pattern was previously obtained using Northern blot analysis (1). The *Ornt3* mRNA, on the other hand, is significantly expressed in CNS tissue, heart, and cultured astrocytes relative to the liver and kidney albeit at a much lower fold difference. In general, the increase in *Ornt3* expression in CNS tissues varied from 1.35-fold in the whole brain to 4.8-fold in the hippocampus relative to the heart (1.0-fold) using *Tbp* as a normalizer. These results confirm and expand previously published Northern blot results of *Slc25a29* in mouse brain and heart (9). A similar pattern of expression was also observed for both *Ornt1* and *Ornt3* after normalizing with *Rpl27* (data not shown) except that *Ornt3* fold differences seen in CNS derived tissues

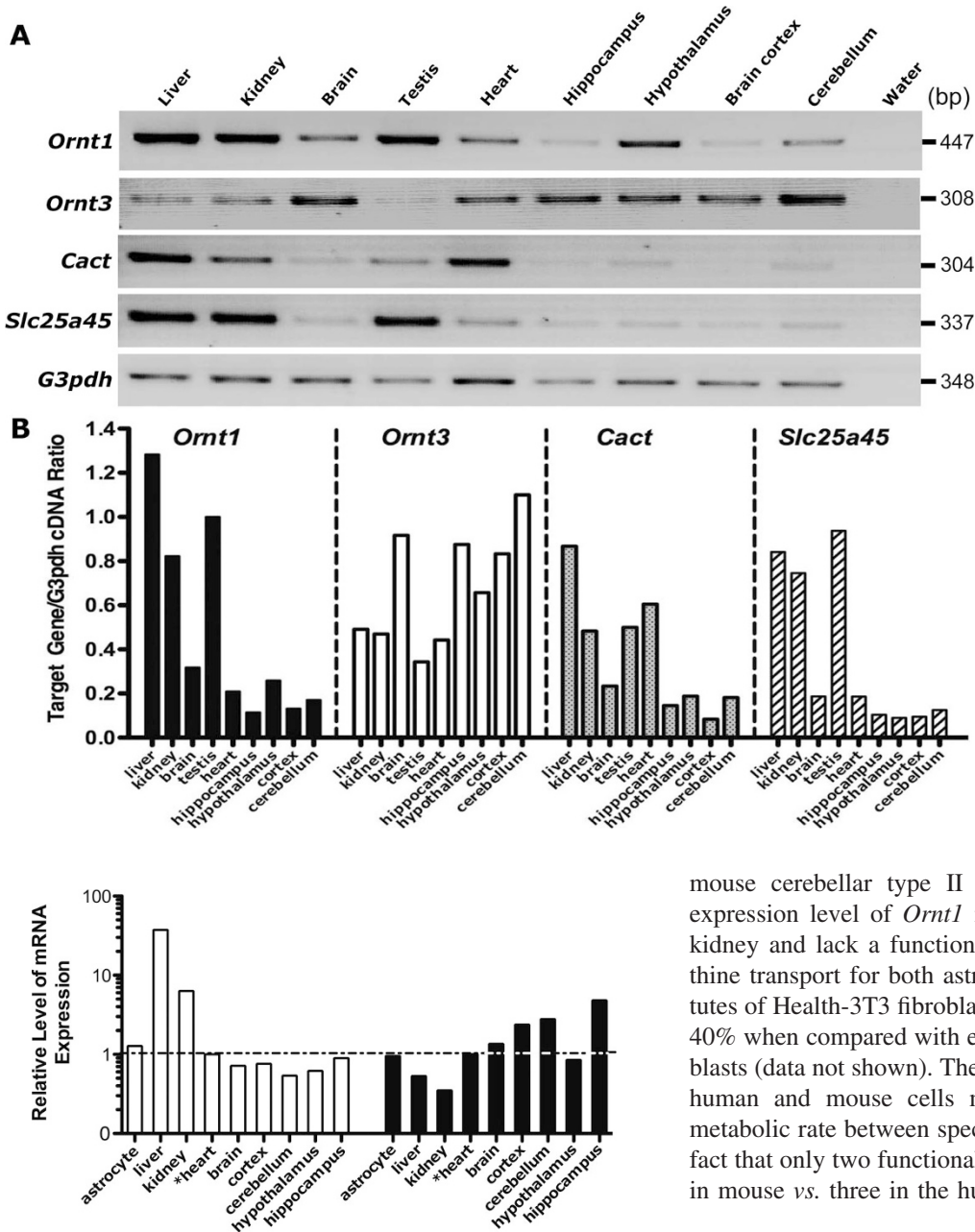


Figure 5. Real time PCR amplification of mouse *Ornt1* (white) and *Ornt3* (black) from peripheral and CNS tissues and cultured mouse astrocytes. We performed qPCR for *Ornt1*, *Ornt3*, and *Tbp* using validated primers and a BIORAD MiniOpticon Real Time Thermocycler. For SybrGreen based amplification, we used 100 ng of first strand DNA synthesized from 2 μ g of total RNA. The C_T values were normalized to those of *Tbp* following the $\Delta\Delta C_T$ method, and the heart was used as a calibrator (*). Figure represents three different experiments performed in duplicate.

were more pronounced (*i.e.*, 3.8-fold in brain and 5.15-fold in hippocampus) with the cerebellum (8.2-fold), not the hippocampus, showing maximum expression. Again, these results were relative to the heart, which was used as a calibrator in all real time PCR experiments (Fig. 5).

Ornithine metabolism in mouse cerebellar astrocytes. Because *Ornt3* is a mitochondrial ornithine transporter that is significantly expressed in CNS tissues, we thought it important to investigate the level of ornithine transport in cultured

Figure 4. Expression pattern of *Ornt1*, *Ornt3*, *Slc25a45*, and *Cact* across mouse tissues. RT-PCR amplification was performed using gene specific primers and commercially obtained total RNA (DNase treated, RNase-free) from different murine tissues. *Panel A* represents 20 μ L of final PCR product run on a 2% agarose gel. *Panel B* represents the ratio of target gene cDNA/*G3pdh* cDNA for each mouse tissue. This figure is representative of experiments performed in duplicate from two different first strand amplifications using 200 ng cDNA per 25 μ L PCR reaction.

mouse cerebellar type II astrocytes, which have a lower expression level of *Ornt1* message relative to the liver and kidney and lack a functional *Ornt2*. Results show that ornithine transport for both astrocytes and mouse National Institutes of Health-3T3 fibroblasts are similar but vary from 30 to 40% when compared with established wild-type human fibroblasts (data not shown). The reason for the difference between human and mouse cells may relate to the differences in metabolic rate between species, variable OAT activity, or the fact that only two functional ornithine transporters are present in mouse vs. three in the humans.

DISCUSSION

In this work, we demonstrate that both the human and mouse *SLC25A29* genes have overlapping function with *ORNT1* and is therefore the third known human mitochondrial ornithine transporter, *ORNT3*. The ability of *SLC25A29* to also function as carnitine/acyl-carnitine translocator-like (CACT) should not come as a surprise given that it is a member of the *ORNT1*, *ORNT2*, *CACT*, and *SLC25A45* subfamily of mitochondrial carrier proteins, which transports positively charged amino compounds. Although the function of *SLC25A45* is unknown, we speculate that it will function as a mitochondrial choline transporter given the very close structural similarity of choline to carnitine (13). Contrary to humans, there are only four functional subfamily members in mice and yeast. In mice, *Ornt2* is nonfunctional; whereas, in yeast, no *ORNT2* exists. The yeast subfamily is composed of

ARG11 (ORNT1 orthologue), CACT, YMC1, and YMC2 (14). Surprisingly, although yeast lacks ORNT2, the existence of a second (redundant) mitochondrial cationic amino acid transport system was reported in the *arg11* KO (14). This suggests that, throughout evolution, gene redundancy for cationic amino acid transport has existed to provide an advantage for species to adapt to metabolic compartmentalization given the very fundamental role of these amino acids transporters in bioenergetics, ammonia detoxification, mitochondrial protein synthesis, and polyamine biosynthesis. Lastly, additional support is the recent characterization of two cationic amino acid transporters (AtmBAC1 and AtmBAC2) in *Arabidopsis thaliana* (15).

SLC25A29's redundant function to CACT, on the other hand, seems to be a more recent evolutionary event. This assertion is based on the observation of lethal phenotypes of *Caenorhabditis elegans* (*dif-1*) and *Drosophila melanogaster* (*Colt*) *Cact* KOs and on the absence of residual transport activity in a yeast *Cact* KO (Δ yor100c) (9,16). Although it is clear that under experimental conditions SLC25A29 works as CACL, it seems that its expression in heart, liver, and brain is not sufficient to have a physiologic effect in the great majority of patients with CACT deficiency who usually succumb to cardiomyopathy and liver dysfunction early in life. In addition to its role in amino acid metabolism, it is possible that SLC25A29 plays a role during embryonic and fetal development because CACT deficient patients do not show any developmental defects unlike the *C. elegans dif-1* and *D. melanogaster colt* mutants. Thus, we speculate that SLC25A29 may also have an important role in structural lipid turnover especially in the brain and heart where it is expressed (9,17).

From a structure-function perspective, it is important to understand how ORNT3 can have overlapping functions with both ORNT1 and CACT. The recent elucidation of the bovine ADP/ATP-1 crystal structure and follow-up work by others has provided some insight into how these transporters may work at the molecular level (8,13). Published conclusions about the solute recognition sites (second, fourth, and sixth TMDs) for both the ornithine and carnitine transporters were deduced using the amino acid structure of the yeast orthologues of these two mitochondrial carriers and other mitochondrial carrier proteins. Given that the findings on the ADP/ATP-1 are based on a monomeric structure, there is always room for subtle but significant differences in these transporters' molecular structure if we consider that they are thought to work as homodimers or possibly as heterodimers (*i.e.*, ORNT1-ORNT3). Perhaps differences in a combinatorial process (protein-protein interactions) mediated in part by post-translational modifications may explain differences in the phenotypic variability of patients with HHH syndrome (3,5).

At the mRNA level, *Ornt3* seems to have higher expression in the CNS when compared with the liver, thus suggesting a potential role for ORNT3 in the CNS cellular pathophysiology of HHH syndrome (9). Although speculative, it may be that ORNT3 serves a compensatory role in CNS tissues by metabolizing excess ornithine accumulated from an ORNT1 deficiency; however, this process could potentially disrupt its

additional role in the CNS metabolism of fatty acids with a secondary effect on brain growth and development. Although the CNS has traditionally been thought of as an organ dependent on ketone bodies, glucose, and lactate as energy sources necessary for growth and development, this notion is starting to change given recent reports, which detail the expression and functionality of components of the fatty acid oxidation pathway in astrocytes (17,18). Our work demonstrated that cultured cerebellar type II mouse astrocytes possess an ornithine transport system that should be physiologically relevant given the fundamental role that cationic amino acids play in brain function. For example, recent work, using a glutaryl-CoA dehydrogenase KO mouse model, highlighted the importance of ORNT1 in brain physiology as it relates to the mitochondrial entry of lysine before its degradation into glutaric acid (19).

To understand the mechanisms of disease underlying the CNS dysfunction variability in patients with HHH syndrome who are under adequate metabolic control, a precise understanding of the biologic functions of ORNT1, ORNT2, and ORNT3 are required. Because ORNT3 transports ornithine *in vitro*, localization of ORNT3 in the periportal hepatocytes will illuminate its potential role in the urea cycle in addition to its likely role in the ornithine oxidation pathway. Liposomal and KO animal studies, however, are needed to elucidate the physiologic relevance of the dual identity of SLC25A29.

Acknowledgments. We thank Greg Merrick for performing all the sequencing and Dario Andrade for technical help. We also thank Dr. Grant Mitchell for the use of HHH fibroblasts.

REFERENCES

- Camacho JA, Obie C, Biery B, Goodman BK, Hu CA, Almashanu S, Steel G, Casey R, Lambert M, Mitchell GA, Valle D 1999 Hyperornithinaemia-hyperammonaemia-homocitrullinuria syndrome is caused by mutations in a gene encoding a mitochondrial ornithine transporter. *Nat Genet* 22:151-158
- Valle D, Simell O 2001 The Hyperornithinurias. In: Scriver CR, Beaudet AL, Sly WS, Valle D (eds) *The Metabolic and Molecular Basis of Inherited Disease*. McGraw Hill, New York, pp 1857-1896
- Camacho JA, Mardach R, Rioseco-Camacho N, Ruiz-Pesini E, Derbeneva O, Andrade D, Zaldivar F, Qu Y, Cederbaum SD 2006 Clinical and functional characterization of a human ORNT1 mutation (T32R) in the hyperornithinaemia-hyperammonaemia-homocitrullinuria (HHH) syndrome. *Pediatr Res* 60:423-429
- Debray FG, Lambert M, Lemieux B, Soucy JF, Drouin R, Fenyves D, Dube J, Maranda B, Laframboise R, Mitchell GA 2008 Phenotypic variability among patients with hyperornithinaemia-hyperammonaemia-homocitrullinuria syndrome homozygous for the delF188 mutation in SLC25A15. *J Med Genet* 45:759-764
- Kim SC, Sprung R, Chen Y, Xu Y, Ball H, Pei J, Cheng T, Kho Y, Xiao H, Xiao L, Grishin NV, White M, Yang XJ, Zhao Y 2006 Substrate and functional diversity of lysine acetylation revealed by a proteomics survey. *Mol Cell* 23:607-618
- Camacho JA, Rioseco-Camacho N, Andrade D, Porter J, Kong J 2003 Cloning and characterization of human ORNT2: a second mitochondrial ornithine transporter that can rescue a defective ORNT1 in patients with the hyperornithinemia-hyperammonemia-homocitrullinuria syndrome, a urea cycle disorder. *Mol Genet Metab* 79:257-271
- Haitina T, Lindblom J, Renstrom T, Fredriksson R 2006 Fourteen novel human members of mitochondrial solute carrier family 25 (SLC25) widely expressed in the central nervous system. *Genomics* 88:779-790
- Palmieri F 2008 Diseases caused by defects of mitochondrial carriers: a review. *Biochim Biophys Acta* 1777:564-578
- Sekoguchi E, Sato N, Yasui A, Fukuda S, Nimura Y, Aburatani H, Ikeda K, Matsuura A 2003 A novel mitochondrial carnitine-acylcarnitine translocase induced by partial hepatectomy and fasting. *J Biol Chem* 278:38796-38802
- de Jonge HJ, Fehrmann RS, de Bont ES, Hofstra RM, Gerbens F, Kamps WA, de Vries EG, van der Zee AG, te Meerman GJ, ter Elst A 2007 Evidence based selection of housekeeping genes. *PLoS One* 2:e898
- Shih VE, Mandell R, Herzfeld A 1982 Defective ornithine metabolism in cultured skin fibroblasts from patients with the syndrome of hyperornithinemia, hyperammonemia and homocitrullinuria. *Clin Chim Acta* 118:149-157

12. Gray RG, Hill SE, Pollitt RJ 1983 Studies on the pathway from ornithine to proline in cultured skin fibroblasts with reference to the defect in hyperornithinaemia with hyperammonaemia and homocitrullinuria. *J Inher Metab Dis* 6:143–148
13. Robinson AJ, Kunji ER 2006 Mitochondrial carriers in the cytoplasmic state have a common substrate binding site. *Proc Natl Acad Sci USA* 103:2617–2622
14. Soetens O, Crabeel M, El Moulaj B, Duyckaerts C, Sluse F 1998 Transport of arginine and ornithine into isolated mitochondria of *Saccharomyces cerevisiae*. *Eur J Biochem* 258:702–709
15. Palmieri L, Todd CD, Arrigoni R, Hoyos ME, Santoro A, Polacco JC, Palmieri F 2006 Arabidopsis mitochondria have two basic amino acid transporters with partially overlapping specificities and differential expression in seedling development. *Biochim Biophys Acta* 1757:1277–1283
16. Oey NA, Ijlst L, van Roermund CW, Wijburg FA, Wanders RJ 2005 dif-1 and colt, both implicated in early embryonic development, encode carnitine acylcarnitine translocase. *Mol Genet Metab* 85:121–124
17. He M, Rutledge SL, Kelly DR, Palmer CA, Murdoch G, Majumder N, Nicholls RD, Pei Z, Watkins PA, Vockley J 2007 A new genetic disorder in mitochondrial fatty acid beta-oxidation: ACAD9 deficiency. *Am J Hum Genet* 81:87–103
18. Blazquez C, Sanchez C, Velasco G, Guzman M 1998 Role of carnitine palmitoyl-transferase I in the control of ketogenesis in primary cultures of rat astrocytes. *J Neurochem* 71:1597–1606
19. Zinnanti WJ, Lazovic J, Housman C, LaNoue K, O'Callaghan JP, Simpson I, Woontner M, Goodman SI, Connor JR, Jacobs RE, Cheng KC 2007 Mechanism of age-dependent susceptibility and novel treatment strategy in glutaric acidemia type I. *J Clin Invest* 117:3258–3270